Printed in U.S.A.

67-HT-60

an ASME publication

$1.50 PER COPY
75¢ TO ASME MEMBERS

Thermal Scaling Applied to Luminous Flames

J. A. COPLEY

Project Engineer,
U. S. Naval Weapons Laboratory,
Dahlgren, Va.

Dimensional analysis has been used to derive a scaling law for evaluating the hea transfer to a body engulfed by large luminous flames. The law consists of elever independent dimensionless variables which must be maintained constant between the model and its prototype. By using the same type of flame in all tests, the scaling law requires principally that (a) the geometrically similar models be fabricated from ma terials whose thermal conductivities are in the same ratio as the length ratio betwee the models; (b) the time scale vary directly as the product of density, specific heat and length; and (c) the internal heat generation vary inversely as the length. A simpl experimental evaluation of the law is also included.

Contributed by the Heat Transfer Division of The American Society of Mechanical Engineer for presentation at the ASME-AIChE Heat Transfer Conference and Exhibit, Seattle, Wash August 6-9, 1967. Manuscript received at ASME Headquarters, June 5, 1967.

Copies will be available until June 1, 1968.

Thermal Scaling Applied to Luminous Flames

J. A. COPLEY

NOMENCLATURE

k = thermal conductivity, Btu/hr ft deg F
$\mathcal{L}$ = characteristic length, ft
$\dot{q}$ = internal heat generation, Btu/hr cu ft
r = position coordinate, ft
t = time, hr
T = temperature distribution, deg R
T_o = initial temperature distribution, deg R
T_f = flame temperature, deg R
α = surface absorptance, dimensionless
γ = surface reflectance, dimensionless
ρC_p = density-specific heat product (volumetric heat capacity) Btu/cu ft deg F
ϵ = surface emittance
ϵ_f = emittance of the flames
σ = Stefan-Boltzmann constant, 0.1714×10^{-8} Btu/hr sq ft deg R^4
C = coefficient of thermal conductance of a joint or thin film, Btu/hr sq ft deg F

INTRODUCTION

The field of heat transfer from large luminous flames is one of growing concern. Recently the various military organizations have directed much effort toward evaluating the response of various items to flame envelopment. Two prominent examples are: (1) ordnance safety, the inadvertent flame envelopment of explosive loaded items; and (2) target vulnerability, the effectiveness of various flame producing weapons against assorted targets. Other areas of flame heat transfer are concerned with the burning and control of large fires. Due to excessive costs, and in most cases irreparable damage, full scale testing in this area has been severely limited. In searching for methods to evaluate flame heating, scale modeling has been investigated as a possible experimental research tool. Thermal scale modeling, or simply thermal scaling, has been used to limited extent to evaluate responses of spacecraft and their various components subjected to solar radiation. The first published work in this area was a 1963 NASA report (1)[1] in which a dimensional analysis approach is used to derive scaling laws and the scaling criteria for the design and testing of thermal models is discussed. Jones (2) and Chao and Wedekind (3) derived general scaling criteria for thermal modeling of spacecraft from governing equations of the system and discussed their practical applications.

The first practical attempt at experimental thermal scaling, as noted by Vickers (4), was made by Clark and Laband (5) who built and tested a one-tenth scale model of a manned orbiting space station. Another one-tenth scale model, that of a solar probe, was built and tested under solar simulation by Lankton (6). Neither of these models was constructed in prototype form and thus the scaling laws have not been verified.

A very thorough treatment of steady-state thermal scaling has been published by Fowle, et al. (7). Here a prototype was constructed and modeled at one-half and one-fifth scales. From these models the authors were able to predict the prototype temperatures within from 1 to 3 percent. This study led to the modeling of the Mariner-Mars spacecraft bus (8). In this investigation a one-half scale model was fabricated and tested by the A. D. Little Co., Inc., while Jet Propulsion Laboratory fabricated and tested the prototype. Results of the data from these tests indicated that 90 percent of the temperatures measured within the model corresponded within 10 F of the temperatures at corresponding points in the prototype.

While thermal scaling for studying steady state phenomena is being reduced to a state-of-the-art technique, its use in studying transient response is far from the like. To the author's knowledge no previous application of thermal scaling has been attempted in the area of flame heat transfer.

THE SCALING THEORY

There are two general approaches that may be taken in order to establish conditions for similitude between a model and its prototype. The first of these is to obtain the dimensionless groups from a set of governing equations and boundary conditions for the system under consideration. The second approach is to obtain the dimensionless groups by dimensional analysis using Buckingham's theorem. This is the approach followed in this paper.

[1] Underlined numbers in parentheses designate References at the end of the paper.

The system to be discussed is an opaque body engulfed in large luminous flames,[2] burning in the open atmosphere. The flames and the outer surface of the engulfed body are considered to be diffuse emitters and absorbers of radiation, and convection is neglected. The flames are assumed to be very large such that their emissivity is independent of flame thickness. The body is considered to be fabricated from homogenous, isotropic materials and the thermal conductivities and specific heats of the materials and assumed temperature independent.[3] The outer surface of the body is considered to be either plane or convex such that it does not radiate to itself. The following phases of heat transfer are considered.

(a) Heat Transfer by Radiation from the Flames

The radiant energy from the luminous flames may be characterized by the flame temperature, the emissivity of the flame, and the Stefan-Boltzmann constant.

(b) Heat Absorbed at the Surface of a Solid

The radiation absorbed at the surface of a solid is primarily dependent upon two factors, the absorptance of the surface, and the total incident flux upon the surface. In the case of the luminous flames and for an object which does not radiate to itself this incident flux is considered to be the radiant energy of the flame and is expressible as $\epsilon_f \sigma T_f^4$.

(c) Radiation Leaving the Surface of a Solid

The radiant energy leaving a surface may be either reflected or reradiated. The parameters characteristic of this energy transfer are the reflectance, and the emissivity, of the surface, as well as the temperature and the Stefan-Boltzmann constant.

(d) Heat Transfer by Solid Conduction

The conduction of heat into a solid is characterized by the conductivity, the temperature distribution of the material, some characteristic length, and a position coordinate in the material. Since transient heating and the resultant variation of internal energy of the material are to be considered, time, the product of density and specific heat (volumetric heat capacity), and the initial temperature distribution must also be included.

(e) Heat Transfer Across a Joint or Film

Across a thin layer of material the transfer of heat follows essentially a steady state law: i.e., $q = C\Delta T$, where C is a reciprocal of thermal resistance to the heat flow, or thermal conductance, the units of which are Btu/sq ft hr deg R and ΔT is the temperature difference across the gap. It is the ratio of the heat transfer across a thin film, or solid-to-solid interface, to the temperature difference across the gap. For joining materials the conductance is a function of the structural characteristics of the joint and the pressure of contact between the two materials. For thin films this conductance is simply the ratio of thermal conductivity to the thickness of the film.

(f) Internal Heat Generation

The heat generated internally within the body is characterized by a single parameter $\dot{q}$, whose units are Btu/hr cu ft.

Buckingham's theorem states that the number of independent dimensionless variables which may be obtained for a system is equal to the number of physical parameters needed to express the behavior of the system minus the number of dimensions required to express the physical parameters. For this case there are 15 physical parameters expressible by four dimensions and therefore 11 independent dimensionless variables will be obtained. The following is one such set.

$$\frac{T}{T_o}, \frac{T_f}{T_o}, \frac{\ell \sigma T_f^3}{k}, \frac{k\,t}{\rho C_p \ell^2}, \frac{\dot{q}\,\ell}{\sigma T_f^4}, \frac{C\ell}{k}, \frac{r}{\ell}, \epsilon, a, \gamma, \epsilon_f$$

Any other grouping of the physical parameters will yield only combinations of the above set.

The first variable, T/T_o is a function of all the others, and this may be expressed in mathematical form as:

$$\frac{T}{T_o} = f\left(\frac{T_f}{T_o}, \frac{\ell \sigma T_f^3}{k}, \frac{k\,t}{\rho C_p \ell^2}, \frac{\dot{q}\,\ell}{\sigma T_f^4}, \frac{C\ell}{k}, \frac{r}{\ell}, \epsilon, a, \gamma, \epsilon_f\right) \quad (1)$$

where f denotes "a function of."

In order to obtain complete thermal similitude between the geometrically similar systems, all of these dimensionless variables must be held constant.

---

[2] Luminous flames as discussed here are flames which derive their luminosity from glowing carbon (soot) particles suspended within the flames. It is the presence of these particles which causes a flame to approach a black body since they radiate continuously throughout the spectrum.

[3] A scaling law has been derived which considers k and C_p temperature dependent, and it is being evaluated at the present time.

SPECIAL APPLICATION

The aforementioned theory is based on strict geometric similarity and is exact for the assumptions considered. However, in most practical applications, restrictions are imposed by Nature upon the physical parameters involved in the dimensionless variables, thereby complicating the fabrication and testing of scale models. It is now worthwhile to discuss the dimensionless variables given in equation (1) and present some methods whereby their constancy between model and prototype may be achieved.

Physical parameters appearing alone in the scaling law as independent dimensionless variables (i.e. ϵ, ϵ_f, a, γ) are required to have the same value for both the model and the prototype. For example, the constancy of ϵ, a and γ could be obtained by coating the model surface with the same material as that which covers the surface of the prototype. The constancy of ϵ_f could be assured by using the same type of flames for both model and prototype tests.

In this analysis the initial temperature distributions within both the model and the prototype are considered uniform and equal. It is possible to extend the scaling theory to include an arbitrary initial temperature distribution; the conclusion being that both temperature distributions must be similar between the model and prototype.

The term $\ell\sigma T_f^3/k$ represents the ratio of the maximum heat flux transferred across a void to that conducted through a material of conductivity, k, and thickness, ℓ, given the same boundary temperatures of T_f and zero. If the models and prototype are subjected to the same type of flames, then for constancy of this term the ratio ℓ/k must remain constant. This requires that the thermal conductivity vary directly as the length scale between the models and prototype. For example, the value of k for the materials used in the fabrication of a one-half scale model must be one half of the value of the prototype. This presents one of the most difficult problems in thermal scaling, since it is not easy to find materials with the proper thermal conductivity from which to fabricate the models. Also, as the models get smaller it may be impossible to find materials with sufficiently low values of conductivity. This condition is particularly troublesome when the prototype contains a good insulating material. A method of slitting the material in a direction perpendicular to heat flow, as discussed by Katzoff (1), may find application here.

The term $kt/\rho C_p \ell^2$ is a Fourier modulus. It represents the ratio of the conducted heat flux to the rate of change of internal energy of the material. If T_f is still assumed constant then the constancy of this term requires that the time scale between the models and prototype be varied as the product $\rho C_p \ell$. For example, if the product of density and specific heat is approximately the same for a one-half scale model and its prototype, then the model will experience a temperature rise twice as fast as the prototype.

The term $\dot{q}\ell/\sigma T_f^4$ represents a ratio of a heat flux due to internal heat generation to that due to radiation. Still assuming T_f constant, the constancy of this term is accomplished by requiring that the internal heat generation, $\dot{q}$, vary inversely as ℓ. Using the half-scale model again as an example, the internal heat generated within the model must be twice that of the prototype. This restriction may not present too great a difficulty in modeling if the heating is due to electrical heating; however, if it is due to chemical reaction such as the thermal decomposition of a propellant or an explosive, then it may be impossible to fabricate a model to include this effect.

The term $C\ell/k$ represents a ratio of the heat transferred across a joint or through a thin film to the heat conducted through a material, given the same temperature difference. Considering the other restrictions which have been imposed on the variation of the physical parameters, the constancy of this term requires that the conductance, C, be the same for both models and prototype. For the case of a thin film on the prototype this would merely require that the film be the same on the models. For a joint, the modeling is more difficult since much is still to be learned about joint conductance.

The term r/ℓ is the ratio of the position coordinate within the body to the characteristic length of the body. It restricts temperatures to be compared only at homologous points within the geometrically similar systems.

EXPERIMENTAL VERIFICATION OF THE THEORY

In order to verify the scaling theory for flame heating (but without internal heat generation), two simply fabricated experimental models, shown in Fig.1, were subjected to heating from large jet fuel fires. The large model was a hollow cylinder, 40 in. long, 11.61 in. od and 10.00 in. id. This was fabricated from a section of AISI 1020 seamless tubing. The second, a 1/2.96 scale model of the first, was fabricated from AISI 304 stainless steel. The scale ratio was determined by selecting an average value of thermal conductivity for each material between the temperature range ambient to 500 F. The variation of

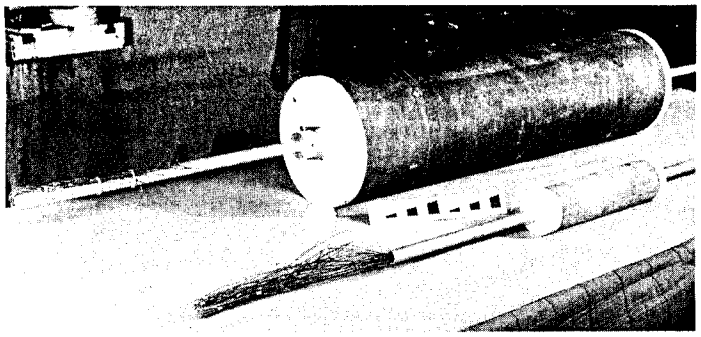

Fig. 1 Instrumented test models prior to flame envelopment

the thermal conductivity ratio from the 2.96 value was ± 10 percent at the extreme ends of the chosen temperature range.

The outer surfaces of both models were ground, polished, and electroplated with pure copper, 0.0002 to 0.0005 in. thick. This thin plating gave both models the same surface radiative properties as dictated by the scaling law while providing a minimum of interference with the conduction of heat into the models. The ends of each cylinder were press-fitted with 2-in. thick disks of asbestos in order to prevent axial heat transfer and thereby approximate an infinite condition in order that later analytical calculations could be facilitated.

Twelve iron-constantan thermocouples were welded on the inner surface of the cylinders in positions that would permit detection of axial and circumferential temperature gradients as well as wall temperature measurements.

A length of small diameter steel pipe was passed through the center of each model. This pipe extended far enough through the cylinder to permit its use as a support for the models within the flames. Drilling holes through the wall of the pipe within the cylinder allowed the thermocouple lead wires to be passed into the center of the pipe and out of the flames without the danger of flame damage to the wires. The pipe was heavily covered with asbestos insulation prior to flame envelopment.

For the flame envelopment, each cylinder was placed on a simply constructed test stand in the center of an 18 ft long by 10 ft wide fuel pan. Water was added to the bottom of the pan to provide a level surface upon which the fuel -- military grade JP-4 jet fuel -- was placed. In each test the surface of the water was 36 in. below the centerline of the test model. One hundred ten gallons, approximately 1 in. depth, of fuel was used in each test. Ignition of this fuel was accomplished by remotely igniting two electric squibs placed in opposite corners of the fuel pan. Exposed junction thermocouples were positioned over the fuel pan at the same horizontal level as the model centerline in order to record flame temperature.

Two motion picture cameras were positioned around the fuel pan to visually determine the uniformity of the flame around the test models.

EXPERIMENTAL RESULTS

Three separate heating tests were conducted on each model. The total burning time of the fuel in each test was approximately 5 min. The motion picture records of the first tests of both cylinders revealed that wind caused the models to be relatively unenveloped by the flames for a major portion of the tests. This resulted in low and erratic temperature records for these tests. For this reason the data of the first tests of both models were not used in evaluation of the scaling law. The motion picture records of the remaining tests on each model showed complete flame envelopment of the models throughout the test.

From the data of the thermocouples within the models it was found that the axial as well as angular variation of temperature over the internal surface of both models was slight. It was also noted that the slope of the temperature time curves of each individual thermocouple in each separate test attained approximately the same value after the initial flame buildup-time. (This slope may be shown to be directly proportional to the heat transfer rate.) Thus, having slopes of approximately the same value strongly suggests that the heat flux over the surface of the model was approximately uniform. For conciseness, the average internal surface temperatures were used to compare the test model data for verification of the scaling law. These data are compared on the dimensionless temperature-time plot, Fig.2. Here the data of both models are separately averaged. The ordinate, T/T_o, is a ratio of absolute temperatures. The thermal conductivity values used for calculation of the Fourier modulus are the same as those used in determining the scale factor. The values of the specific heats were taken in the range 200-250 F to correspond to the midpoint of the temperature range over which the larger cylinder was tested. The values of the thermal properties were taken from reference (9). The characteristic length, ℓ, is the wall thickness of the cylinders.

DISCUSSION OF EXPERIMENTAL RESULTS

Two points require explanation in Fig.2: First, the flattening of the curves at different

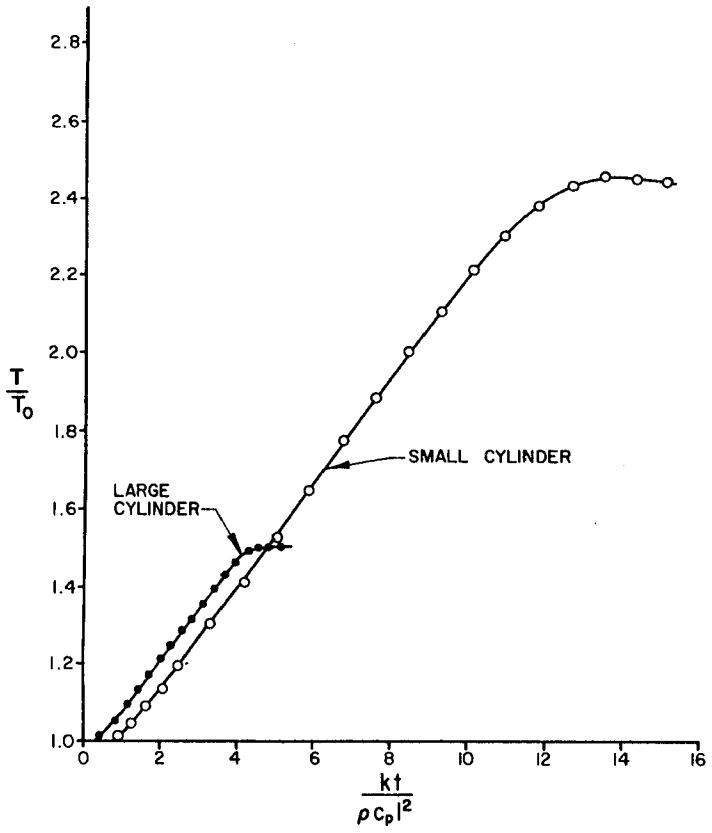

Fig. 2 Graph showing dimensionless temperature-time data

points, and second, the zero shift in the origin of the curves. Both points are related through the variation of the time scale and the finite buildup and burning time of the flame and may be easily explained.

First, the flattening of the curves is a result of the decrease in flame intensity due to the finite flame burning time. For this flattening to have occurred at the same dimensionless time point on each model, the flames should have burned approximately one-third as long for the smaller model or three times longer for the larger model. This is determined by the ratio $(\rho C_p \ell)_1/(\rho C_p \ell)_2$ where the subscripts refer to the different size models.

Second, the zero shift of the curves is the result of the buildup-times of the flames being approximately fixed for both models. For these curves to have had the same origin the flame buildup-time should have been approximately three times longer for the larger model or one third as long for the smaller. A zero buildup-time flame in the test of both models would also start the curves at the same origin. Again, since the time scale must vary as the product $\rho C_p \ell$, any fixed or common time to both models will cause a separation of the curves.

Since scaling of the buildup and burning times of the flames was not attempted in these series of tests, the dimensionless temperature-time plots of the data should be compared on the basis of their slopes for verification of the scaling law.

The effect of the wind has been excluded from this investigation by discarding the data of those tests so affected. If the effect of the wind is to be considered in the transient response of some item subjected to flame heating, then it will be necessary to include additional variables into the scaling law which may preclude thermal scaling. Eliminating the effect of the wind in this investigation should have provided data which represented approximately the maximum thermal response of the test models.

The plating of both models to insure equal radiant surface properties may not have been necessary, since the cylinders rapidly coat with soot in the flames. Thus, the emittance of the plating on the surface of the models would be a factor in the radiant heat transfer for a short time or until the surface was thoroughly coated with soot. The actual time required to thoroughly coat the models with soot is not known, but tests conducted previous to the actual taking of data reveal that this time is somewhere in the neighborhood of the buildup-time of the flames, or approximately 20 sec from the time of fuel ignition. The thickness of this soot layer was approximately 0.002 in. at the end of each test. By considering the soot layer as a thin film, the conductance, C, remained the same for both models and consequently the scaling law is automatically satisfied.

CONCLUSIONS

From the equality of the slopes of the curves in Fig.2 it is evident that the response of the test models did follow the scaling law and that the scaling of the heat transfer from luminous flames is possible. However, it is also evident, as this simple experiment shows, that for this scaling law to be correctly applied, care must be taken to assure the proper time scaling of the buildup of the flames as well as their duration.

At the present time a method has not been developed whereby the buildup-time of flames, such as described in this paper, may be controlled. However, for cases in which the buildup-time of the flames may be considered zero, such as flames from incendiary bombs or flame throwers, the use of this scale modeling technique without further refinement would definitely provide a simple and economical means of evaluating the transient response of an item engulfed by such flames, pro-

viding materials may be found with the proper thermal properties from which to construct the models.

ACKNOWLEDGMENTS

The author wishes to express his appreciation to Dr. William G. Soper of the U. S. Naval Weapons Laboratory for his valuable assistance and suggestions throughout this research.

REFERENCES

1 S. Katzoff, "Similitude in Thermal Models of Spacecraft," NASA TN D-1631, 1963.

2 B. P. Jones, "Thermal Similitude Studies," Journal of Spacecraft and Rockets, vol. 1, no. 4, 1964, pp. 364-369.

3 V. T. Chao and G. L. Wedekind, "Similarity Criteria for Thermal Modeling of Spacecraft," Journal of Spacecraft and Rockets, vol. 2, no. 2, 1965, pp. 146-152.

4 J. M. Vickers, "Thermal Scale Modeling," Astronautics and Aeronautics, vol. 3, no. 5, May 1965, pp. 34-39.

5 L. G. Clark and K. A. Laband, "Orbital Station Temperature Control," Astronautics, vol. 7, no. 9, 1962, pp. 40-43.

6 C. S. Lankton, G. E. Missiles and Space Division, personal communication.

7 A. A. Fowle, et al., "Thermal Scale Modeling of Spacecraft: an Experimental Investigation," Author D. Little, Inc. report to Jet Propulsion Laboratory, June 28, 1963.

8 F. Gabron and R. W. Johnson, "Thermal Scale Modeling of the Temperature Control Model of Mariner Mars 64," Author D. Little, Inc. report to Jet Propulsion Laboratory, January 25, 1965.

9 T. Lyman, Metals Handbook, Cleveland, American Society for Metals, 1961.

Zongi + 5779

Journal of Hazardous Materials, 20 (1988) 21–40
Elsevier Science Publishers B.V., Amsterdam – Printed in The Netherlands

Heat Transfer to Large Objects in Large Pool Fires

B. L. Bainbridge and N. R. Keltner

Thermal Test and Analysis Division(7537), Sandia National Laboratories, P. O. Box 5800, Albuquerque, New Mexico, 87185 (USA)

Summary

A series of large pool fires has provided temperature and heat flux data for a large, thermally massive object. Tower temperatures were obtained at 4 elevations. Temperature measurements on a large calorimeter were used to obtain heat flux levels at 3 axial stations and 4 angular locations. The tests show large spatial and temporal variations for each test that seem to be largely driven by wind effects. A conditioning analysis was used to extract data at periods of lower wind velocities to allow a comparison between test data and simplified fire models. The conditioned data shows a significantly lower variance and better symmetry around the large calorimeter.

Introduction

Large pool fires are used at Sandia National Laboratories to expose radioactive material shipping containers to levels of temperature and heat flux required by regulatory agencies. Due to the very nature of outdoor pool fires, a large effort has gone into characterizing the temporal and spatial variability of the thermal environment.

Three tests were performed in the summer of 1983 involving a 9.1 by 18.3 meter pool fire fueled with JP-4 aviation fuel. A calorimeter 1.4 m in diameter by 6.1 m long was used to examine the thermal input to a relatively large, massive object. An examination of temperature and heat flux data emphasizes the effect of even low wind conditions on the overall structure of the fire. In an attempt to examine the thermal environment in the absence of any disturbances, a 'conditioning signal' was used to extract data during periods of low wind.

Heat flux and temperature data obtained from the large pool fire tests is presented and the variation over the surface of the large calorimeter is examined. The application of a conditioning signal is used to reduce the wind induced variance in the heat flux data.

Fire Test Regulations

Fire tests are typically specified as either a temperature versus time curve or as the equivalent of a radiant environment at a specific temperature. An example of the former is provided by the American Society for Testing and Materials(ASTM) in test method E 119, "Standard Methods of Fire Tests of Building Construction and Materials"[1]. The latter specification is used by several agencies that have regulations regarding the fire testing of radioactive material transportation containers. In general, the requirements involve a 30 minute test with the thermal environment equivalent to a radiant source of 1075K with an emissivity of at least 0.9 and a surface absorptivity for the test item of 0.8 or greater. A convective component should be equivalent to still air at 1075K. The specific regulations are available in publications from the agencies themselves:

a. the Department of Energy(DOE)[2], orginally published by ERDA, in chapter 0529 of the ERDA manual "Safety Standards for the Packaging of Fissile and Other Radioactive Materials",
b. the Department of Transportation(DOT)[3] in the Code of Federal Regulations(CFR) as 49 CFR Part 173,
c. the Nuclear Regulatory Commission(NRC)[4] in 10 CFR Part 71,
d. the International Atomic Energy Agency(IAEA)[5] published in IAEA Safety Standards, Safety Series No. 6, "Regulations for the Safe Transport of Radioactive Materials".

A more severe test requirement, E-5 P-191 entitled "Determining Effects of Large Hydrocarbon Pool Fires on Structural Members and Assemblies", has been proposed by the ASTM[6] for evaluating fire protection materials for the petrochemical industry. It requires a thermal environment equivalent to a 1290K source with a 10% convective component. Also stipulated is the rapid development of both high temperatures and heat flux levels in order to impose the thermal shock effects that are produced in actual fire environments.

Test Instrumentation

The three pool fire tests were conducted in a 9.1 by 18.3 by 0.9 meter concrete pool. The 30 minute tests used a layer of JP-4 fuel, approximately 0.22 m thick, that was floated on 0.66 m of water. Instrumentation was mounted in 8 towers, 4 small calorimeters(0.1 m and 0.2 m diameter) and 1 large calorimeter(1.43 m diameter). Data obtained from the large calorimeter is of

primary interest. Figure 1 shows the relative locations of the instrumentation.

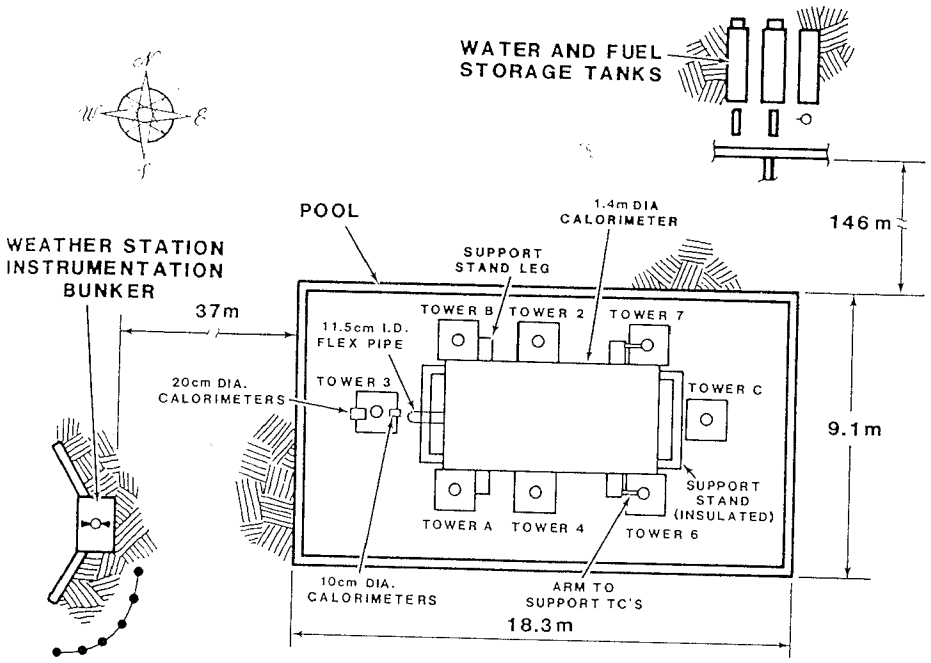

Figure 1. A diagram of the large pool fire facility. Shown are the relative locations of the large calorimeter and towers.

The large calorimeter consisted of a 10 tonne cylinder that was 6.4 m long and 1.4 m in diameter. The 3.2 cm thick walls were of A517 steel and reinforced by 5.1 cm thick ribs located on 61 cm centers. The ends of the cylinder were sealed with plates 1.3 cm thick. The interior of the calorimeter was insulated with 3 layers of 2.5 cm thick material that were held in place with a steel mesh.The large calorimeter was centrally located with its lower surface 0.9 m above the pool surface. Figure 2 shows the physical layout of the large calorimeter.

Type K thermocouples were mounted at 3 axial stations on the large calorimeter: in the middle and at 0.46 m from both ends. At each station, thermocouples were mounted at 4 angular locations: 0(bottom), 90(south), 180(top), and 270(north). At least 3 thermocouples were located at each of the 12 measurement locations. One was mounted between the first and second layers of insulation, the next was an intrinsic thermocouple welded to the inner surface of the cylinder wall, and an exterior thermocouple was mounted with the junction approximately 5 cm from the outer surface(see figure 2). The interior

thermocouples are used to calculate net heat flux and the exterior measurement is used to monitor flame temperatures near the calorimeter surface.

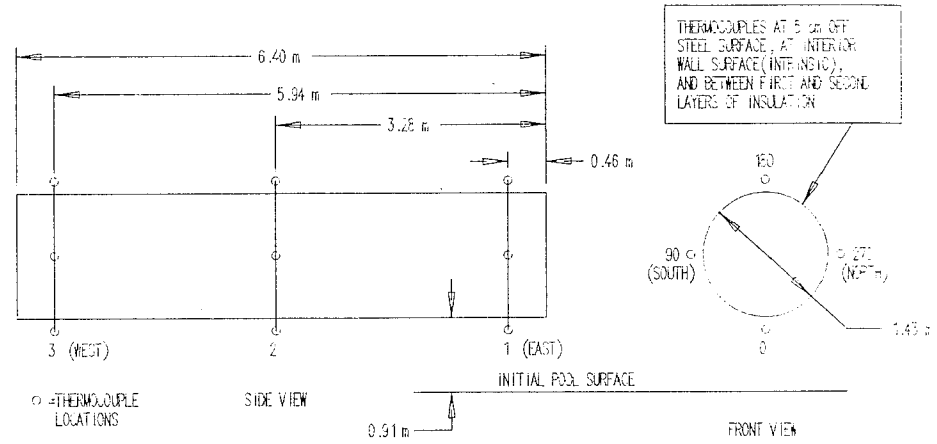

Figure 2. A schematic of the large calorimeter. The axial and circumferential thermocouple locations are shown. Note the cross section that depicts the external, surface, and internal thermocouples.

Temperature measurements in the fire environment were obtained using type K thermocouples mounted on several towers within the pool(figure 1). Towers A, B, and C were 6.1 m in height with measurement stations at 1.42 and 2.62 m above the initial fuel surface. The other 5 towers were 12.2 m tall with thermocouples mounted at 1.42, 2.62, 5.49 and 11.18 m. At all locations, sheathed thermocouples with ungrounded junctions were used.

The data acquisition system consisted of a Hewlett-Packard(HP) 3052A data logger connected to an HP-21 MX computer using fiber optic cables. All channels were recorded every 4.5 seconds. In order to monitor the integrity of the thermocouple channels, a resistance measurement was substituted for the temperature measurement every tenth reading.

Additional details regarding the test instrumentation are available from reference 7. Included is information on the small calorimeters and wind velocity measurements.

Results

Temperature Measurements

A complete presentation of all the data recorded during the 3 pool fire tests is beyond the scope of this paper. Representative samples of temperature and heat flux data will be presented with an emphasis placed on examining the variability of heat flux levels. A more complete report is presented in reference 7.

The primary cause of large fluctuations in the fire environment is wind. It induces changes in the mixing and combustion of fuel and air and in the resulting thermal profiles above the fuel surface. The regions of flame above a fire shift location as a function of the wind velocity and the buoyancy induced flow within the fire. Figure 3 shows a sample of recorded wind speed and direction from the third test(test C). The steady rise in speed coupled with the shift in direction of 180 degrees produces a fairly unpredictable environment. Objects in the fire are alternately engulfed in flame and exposed to ambient air.

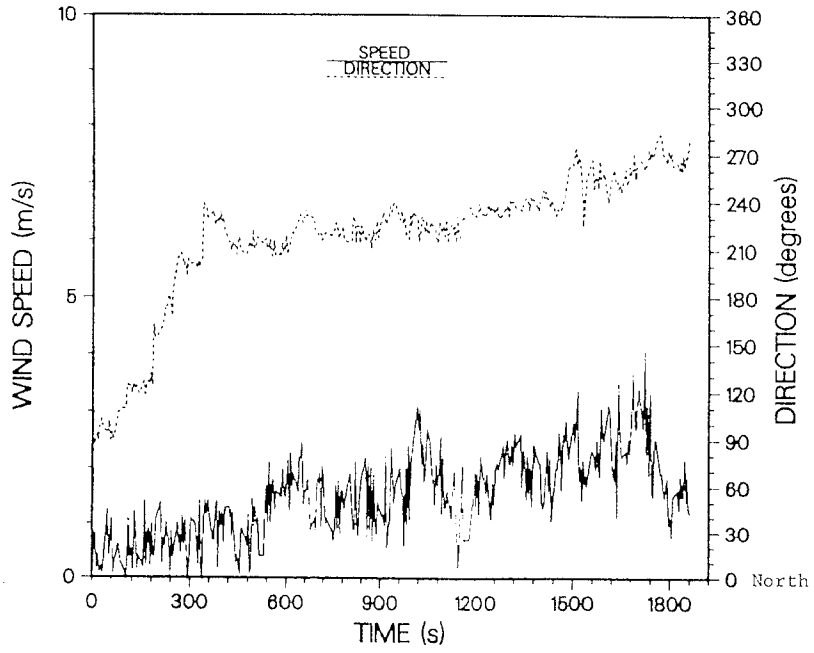

Figure 3. A sample wind velocity plot from test C. The upper trace shows wind direction and the lower wind speed. Note the 180 degree wind shift over the course of the test.

Temperatures recorded from the tower instrumentation clearly show the large fluctuations experienced during the three tests. Figure 4 is a representative sample of temperature versus time for tower 6(see figure 1) of test A. The temperatures are shown at all 4 heights: from 1.42 m to 11.18 m. While the trend was for lower temperatures with increasing height, there were some periods when all locations registered similar temperatures(1600 to 2000 seconds).

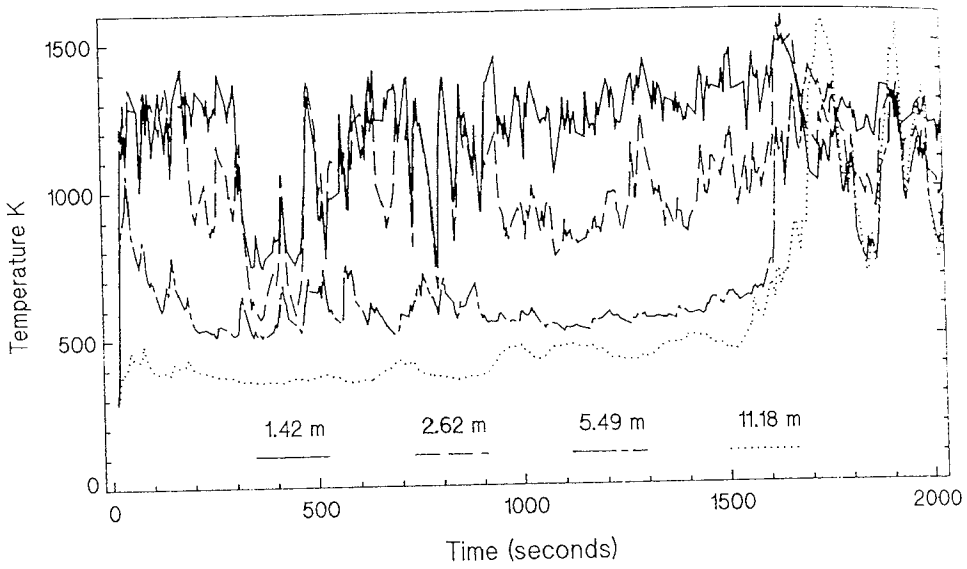

Figure 4. Tower temperature versus height for test A, tower 6.

Another example of the variance in the fire temperature data may be seen in figure 5, where temperatures are plotted for 3 different towers at the same elevation from test C. Tower B has a significantly higher average temperature than the other two. In fact, the difference in temperature approaches 800K. Obviously, the fire was highly asymmetric for most of the test duration.

Tower temperatures are useful for examining the gross fire structure and providing insight regarding the highly variable nature of the temperature profile and heat loads. Table 1 is a compilation of average and standard deviations for tower temperatures recorded during all three tests. Note the decreasing average and increasing standard deviation with increasing elevation. Even at the lowest elevation, 1.42 m, the standard deviation is 20% and it increases to over 60% at 11.18 m. As a result of these large variations, objects within the fire could see heat loads that would vary by a factor of two or more depending on location.

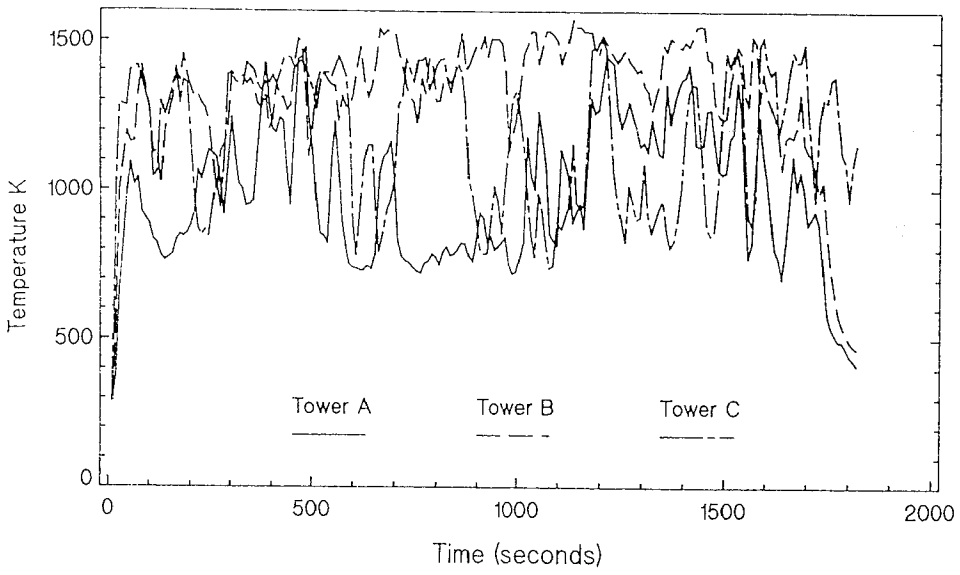

Figure 5. Tower temperatures recorded from test C for 3 different towers. The thermocouples were located at 2.62 m above the initial fuel level.

TABLE 1
Tower temperatures and statistics for tests A, B, and C. The values represent averages obtained over the entire test. Note: the information in this table was obtained from reference 7.

Location	Test A	Test B	Test C
Elevation 1: 1.42 m			
Minimum (K)	588	715	446
Maximum (K)	1595	1532	1546
Average (K)	1142	1194	1231
Standard Deviation	24%	21%	18%
Elevation 2: 2.62 m			
Minimum (K)	393	507	414
Maximum (K)	1575	1572	1581
Average (K)	992	1031	1094
Standard Deviation(%)	37%	35%	32%
Elevation 3: 5.49 m			
Minimum (K)	346	382	397
Maximum (K)	1529	1539	1564
Average (K)	767	829	812
Standard Deviation(%)	52%	48%	51%
Elevation 4: 11.18 m			
Minimum (K)	342	362	326
Maximum (K)	1566	1494	1507
Average (K)	649	676	667
Standard Deviation(%)	70%	61%	65%

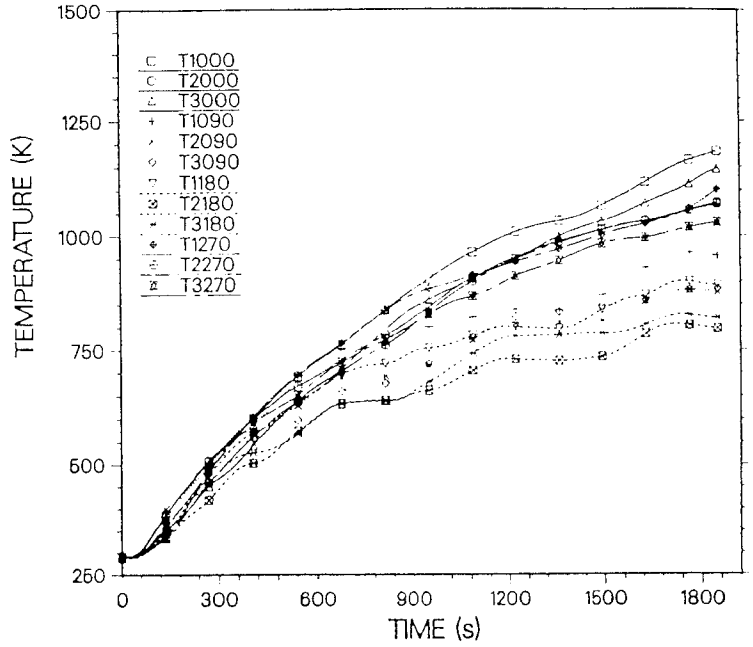

Figure 7. Temperatures measured at the inside surface of the large calorimeter wall for test B.

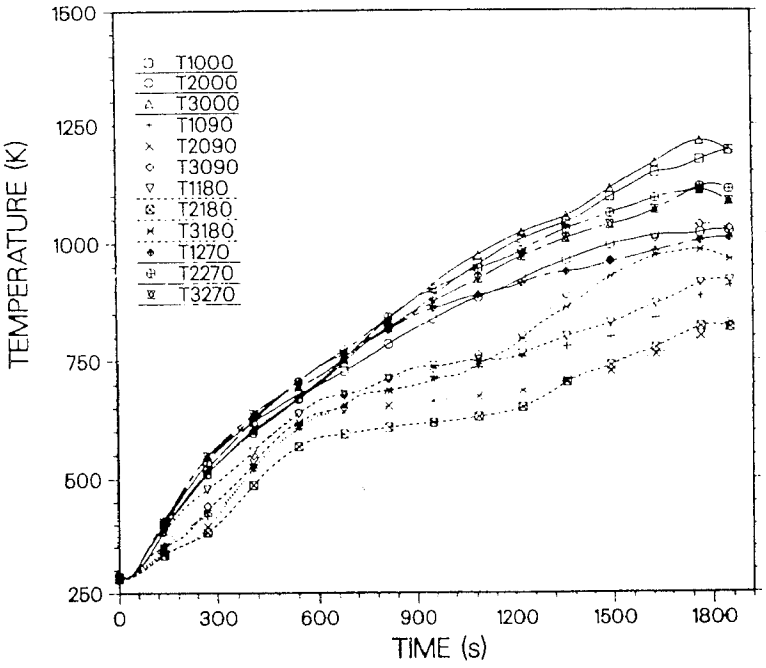

Figure 8. Temperatures measured at the inside surface of the large calorimeter wall for test C.

The large calorimeter provided temperature and heat flux data that is representative of heat loads that would be seen by a massive object in a pool fire. Data recorded from intrinsic thermocouples mounted on the inner surface of the calorimeter wall show the variation in heat loads at different points on the calorimeter body. Figures 6, 7, and 8 show the magnitude of the variation for tests A, B, and C, respectively. An indication of the source of the variance in the data can be seen by comparing the temperatures at 90(south) and 270(north) degrees. In a steady fire environment, a centrally placed object would experience a heat load that would be uniform around the object at a given elevation. As the figures show, the 90 degree locations tend to be much lower than the measurements at 270 degrees. This correlates with the light winds that usually were from the southeast or southwest directions.

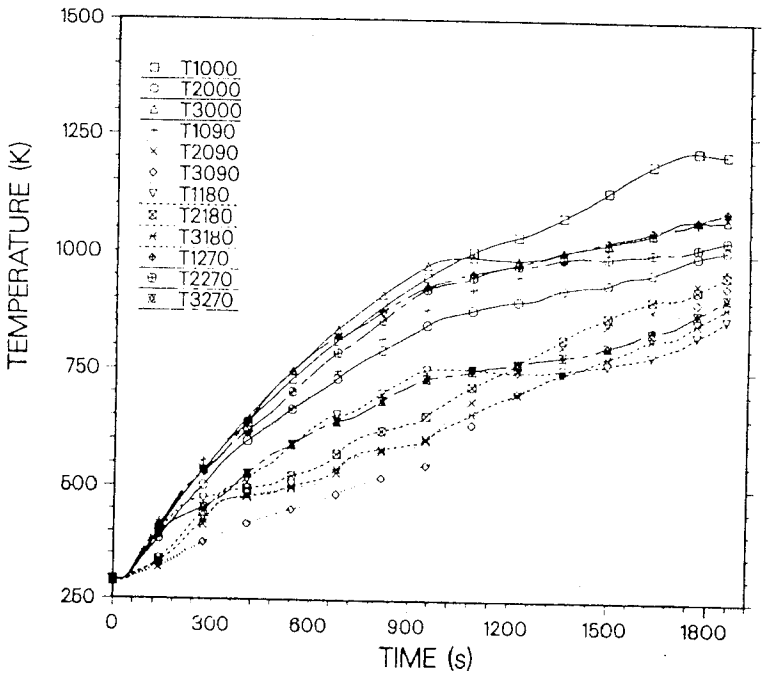

Figure 6. Temperatures measured at the inside surface of the large calorimeter wall for test A.

Heat Flux Measurements

The inner surface temperature measurements were used to calculate net surface heat flux for the large calorimeter. A one dimensional inverse heat conduction program, SODDIT(Sandia One Dimensional Direct and Inverse Thermal)[8], was used with a simple model of the calorimeter wall. Temperature

dependent material properties were included. Stability requirements necessitated the use of 4 future times(4 successive data points) for the inverse calculation. This also tends to smooth the data and reduce the noise levels of the resulting output.

One problem with the heat flux calculation was caused when the A517 wall material reached its Curie point(1033K). The abrupt change in thermal properties caused instabilities in the calculated heat flux that are seen as sinusoidal fluctuations . The transition point was reached at different times near the end of the test depending on the temperature history experienced at a particular station on the large calorimeter. A typical point was near 1600 seconds into the test.

Figures 9 and 10 show representative results for test C at station 2, locations 0 and 180, respectively. The inner wall temperature, external gas temperature, and calculated heat flux are all shown as functions of time. Note the difference in frequency content of the three signals. The inner wall temperature changes only very slowly with time and doesn't reflect the rapid fluctuations in the adjacent gas temperature. The calculated heat flux, which is responsive to the derivative of the inner wall temperature, does show some correlation with the gas temperature trace. Note that the negative slope in

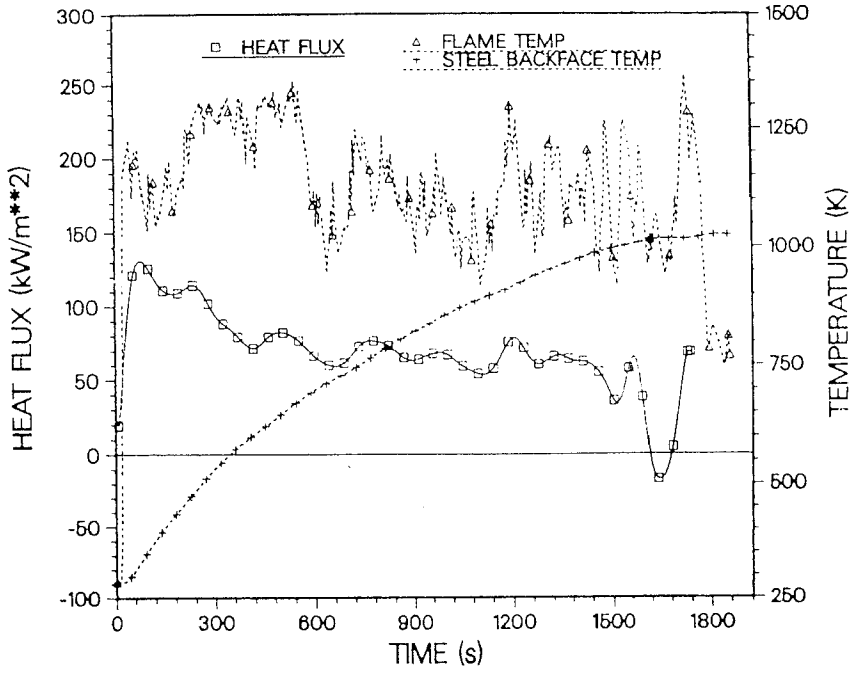

Figure 9. Heat flux, flame temperature and backface temperature for the large calorimeter during test C, station 2, 0 degrees.

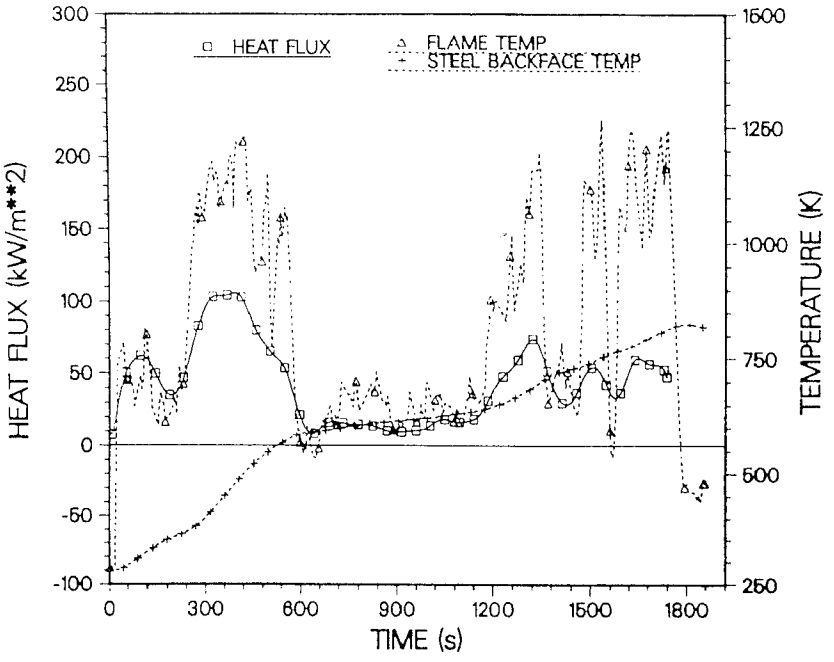

Figure 10. Heat flux, flame temperature and backface temperature for the large calorimeter during test C, station 2, 180 degrees.

figure 9 was due to the rising temperature of the exterior wall of the large calorimeter, which reduced the net heat flux to the wall.

A comparison between figures 9 and 10 shows the large point to point variation in heat flux experienced by the large calorimeter. While the heat flux at 0 degrees remained fairly constant, the more exposed 180 degree location exhibited large changes in heat flux that correlate well with the fluctuations in external gas temperature. This same situation existed for all three tests.

An important aspect of the thermal environment of a fire concerns the distribution of heat flux with location. Fire models typically predict the highest heat flux for the upper surfaces of the cylindrical calorimeter. There has been speculation about the existence of a fuel rich vapor dome near the surface of a large fire[9], although other authors predict its presence only for small(<1 m) diameter fires[10]. The existence of a vapor dome would reduce the heat flux to the lower surface of the calorimeter in accordance with the models. Simplified radiation models base the varying heat flux on the optical path length in a fire and the proximity of the cooler fuel surface to the lower surfaces of an object[11]. To examine the performance of those models, the heat flux histories were averaged over the 3 stations for each test and plotted in figures 11 through 13.

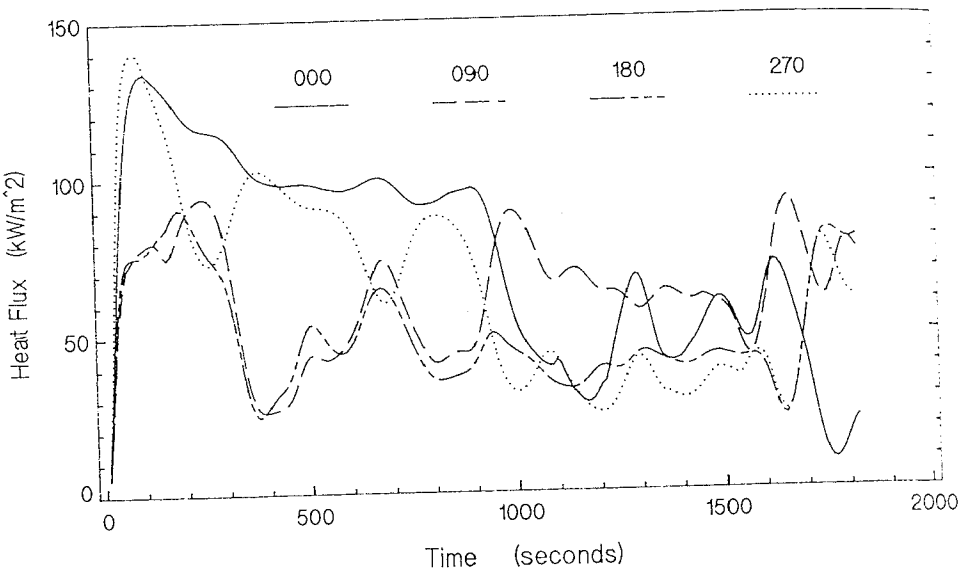

Figure 11. Heat flux versus time for test A. The data was averaged over 3 axial stations.

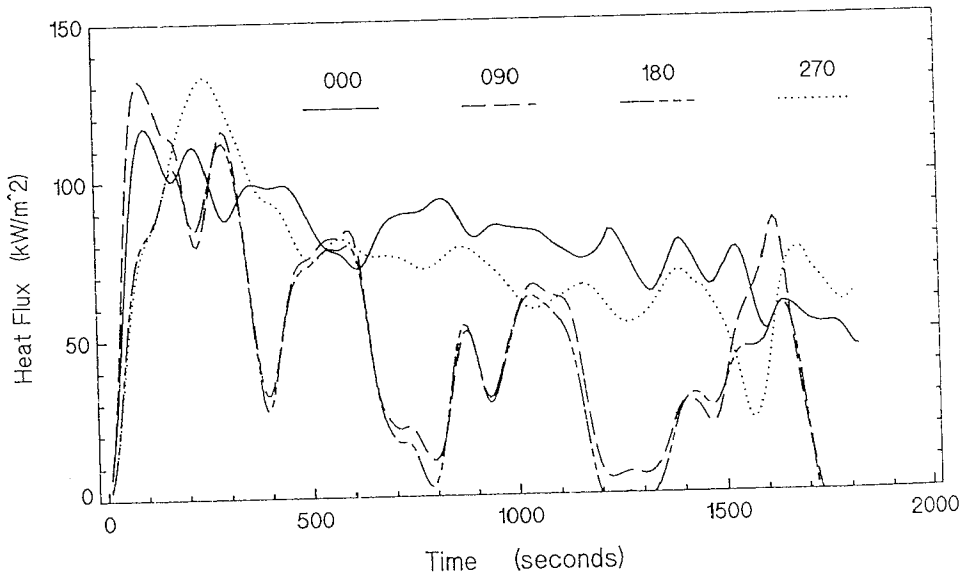

Figure 12. Heat flux versus time for test B. The data was averaged over 3 axial stations.

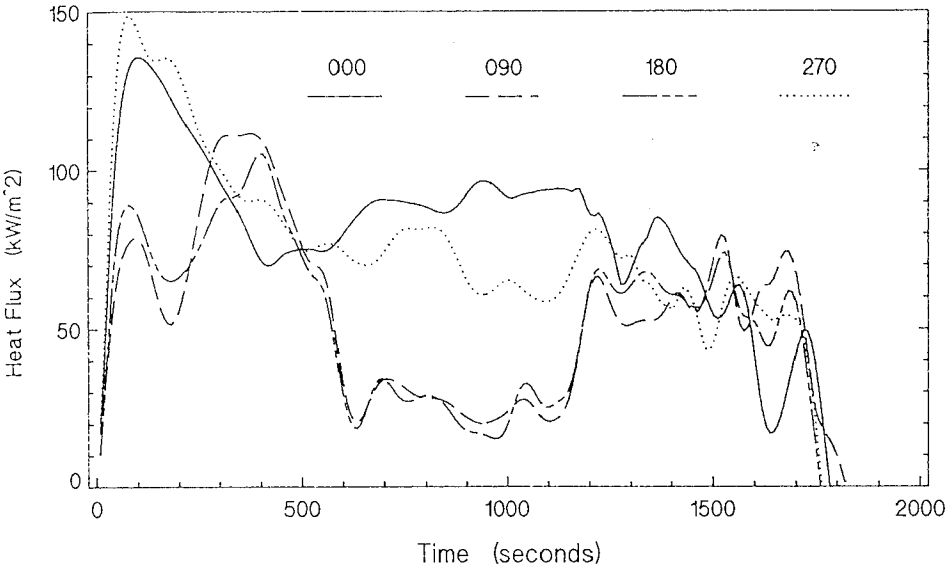

Figure 13. Heat flux versus time for test C. The data was averaged over 3 axial stations.

In all three tests, the data divides itself into two groups: 0 and 270 locations and 90 and 180 locations. This is expected from the generally southerly wind direction experienced during the tests. In other words, the dominant features of the heat flux profiles are wind induced. The variation by angular location is more clearly shown in figures 14 and 15. The total heat flux was estimated by adding a radiated surface heat flux component(emissivity=0.85) to the calculated net heat flux for a given location on the large calorimeter. The total heat flux becomes fairly stationary from a statistical standpoint and the calculated mean value for a given test is more significant. The variation in figure 14 shows the reduction in heat flux for the 90 and 180 locations. The standard deviations for the mean total heat flux values are also greater for the more exposed locations.

A casual inspection of the data seems to indicate a situation opposite to that predicted by the models: the lowest location(0 degrees) has the highest average heat flux while the highest location(180 degrees) has one of the lowest averages. A closer examination shows that the magnitude of the variance in the heat flux data, caused by wind effects, makes it difficult to interpret the distribution of heat flux with location. The data cannot be used in its present form to evaluate the veracity of a particular fire model.

Due to the specification of a fire environment in terms of its radiant equivalent, it is sometimes convenient to present the heat flux data as a function of the surface temperature of the object being tested. Figure 16

shows the heat flux versus calorimeter surface temperature(calculated) averaged over three tests. The behavior as a function of angular location is similar to the plot of heat flux versus time; namely, the 90 and 180 locations show good agreement as do the 0 and 270 locations.

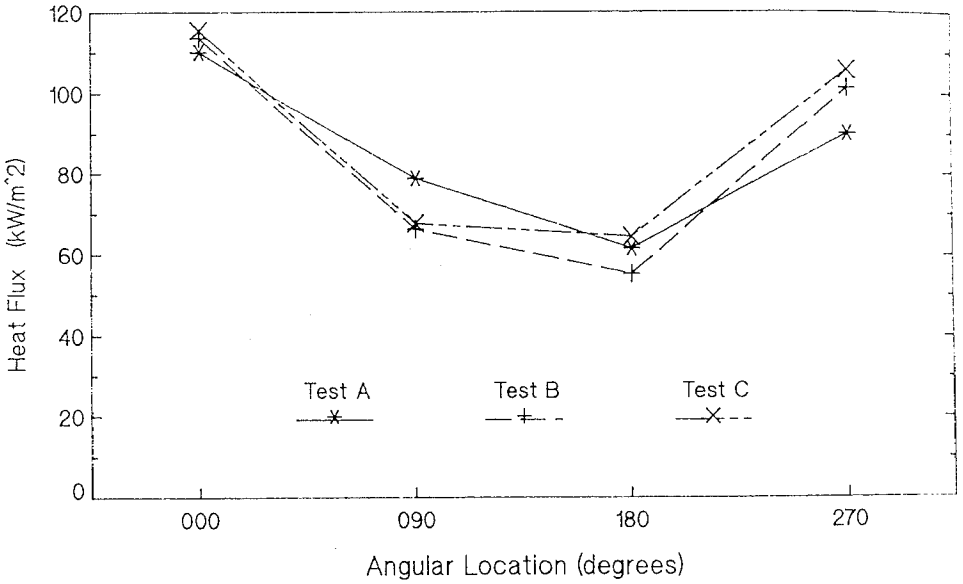

Figure 14. Average total heat flux versus angular location for tests A, B, and C.

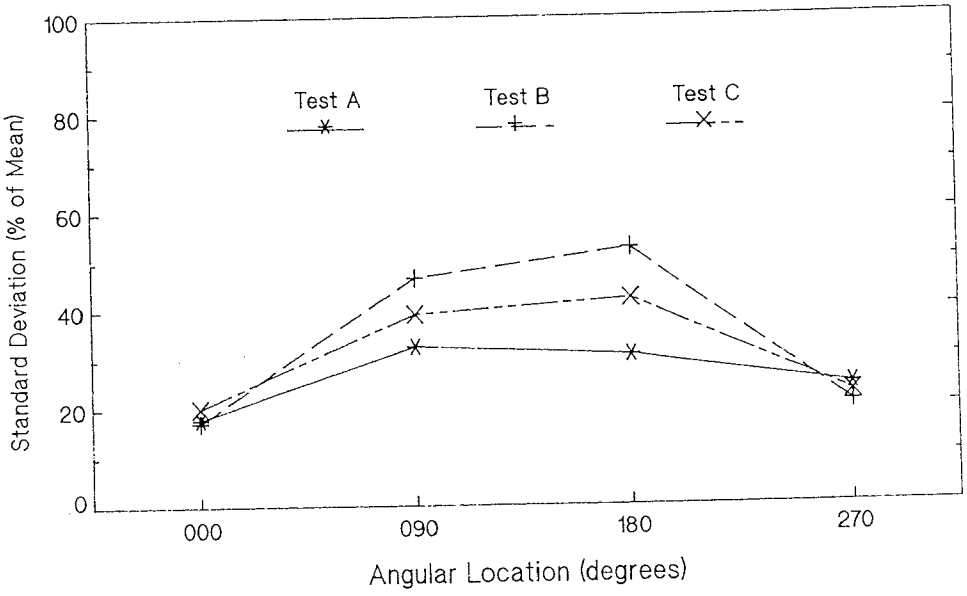

Figure 15. Standard deviations of the average total heat flux versus angular location for tests A, B, and C.

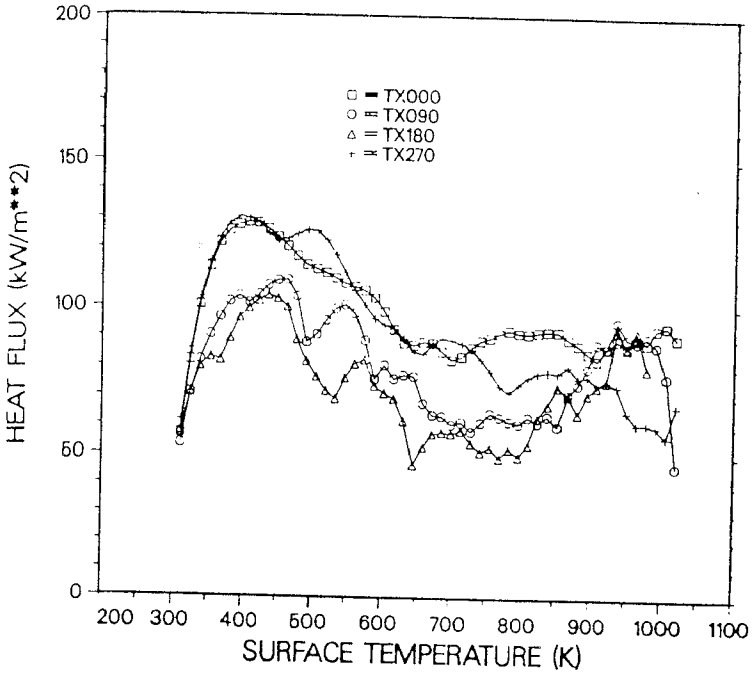

Figure 16. Heat flux versus surface temperature for the large calorimeter. The data was averaged over the three tests and plotted for each angular location.

Conditional Sampling

Fire models assume the existence of a steady fire environment. It is not possible, at present, to add a non-steady wind component that would allow a comparison to test data. It is desirable, instead, to remove or reduce the impact of data that was recorded during periods of 'significant' wind velocities. Several methods are possible, but one that has been successful is based on the use of tower temperatures to conditionally sample the data. The technique has been employed successfully in the analysis of fire velocities and temperatures[12].

Figure 1 shows that the large calorimeter was surrounded by towers. If an appropriate temperature was selected, it should be possible to examine the data and surmise when a tower was engulfed in flame. If an upwind tower was used, the engulfment of the tower would be an indication of a low wind condition and it would be assumed that the calorimeter was also engulfed. The first difficulty is selecting the temperature for a given height and tower that is an indication of the desired fire condition.

A distribution of all the tower temperatures registered at elevation 2 for all three tests was obtained. Figure 17 shows that the distribution was bimodal: one peak near 730K and another near 1230K. The second peak is assumed

to be the mean value of a second normal distribution that is an indication of a flame present condition. A cutoff temperature of 1040K was used as a conditioning criterion for heat flux data from the large calorimeter to restrict the data set to periods of time when the tower temperatures indicate engulfment. Data was not used if obtained during periods when the upwind tower temperature was below the cutoff point. It was hoped that the wind induced variance in the heat flux data would be reduced.

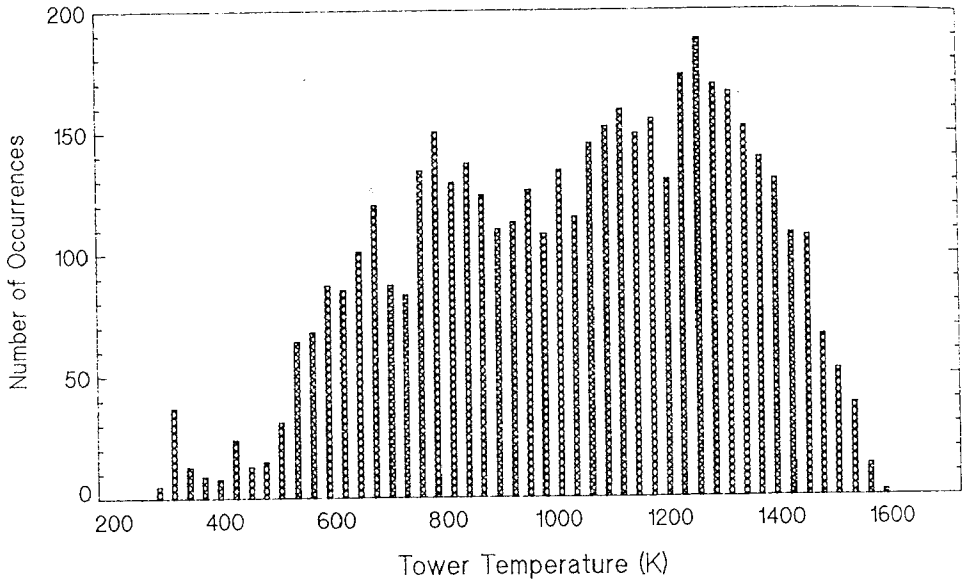

Figure 17. The frequency distribution of tower temperature at 2.62 m. Note the bimodal distribution.

For each test, the flame present temperature was used in conjunction with the data from tower 6, elevation 2, to condition the heat flux data(figures 11 through 13). The results are shown in figures 18 through 20. The heat flux data seems to have a lower variance, especially for the 90 and 180 locations. The effect of conditioning on the statistics is more obvious when presented as a test mean and standard deviation, as was done for the original data set(figures 14 and 15). Again, total heat flux was used and the results plotted in figures 21 and 22. The mean heat flux values begin to show the type of symmetry that would be expected in a steady fire environment: agreement between 90 and 270 locations and the steady change in magnitude from the lowest to highest locations on the calorimeter. Note that the standard deviations are, as expected, much lower for the 90 and 180 locations after being conditioned. The trend in heat flux with location again indicates that the highest values would be found at the bottom of the calorimeter.

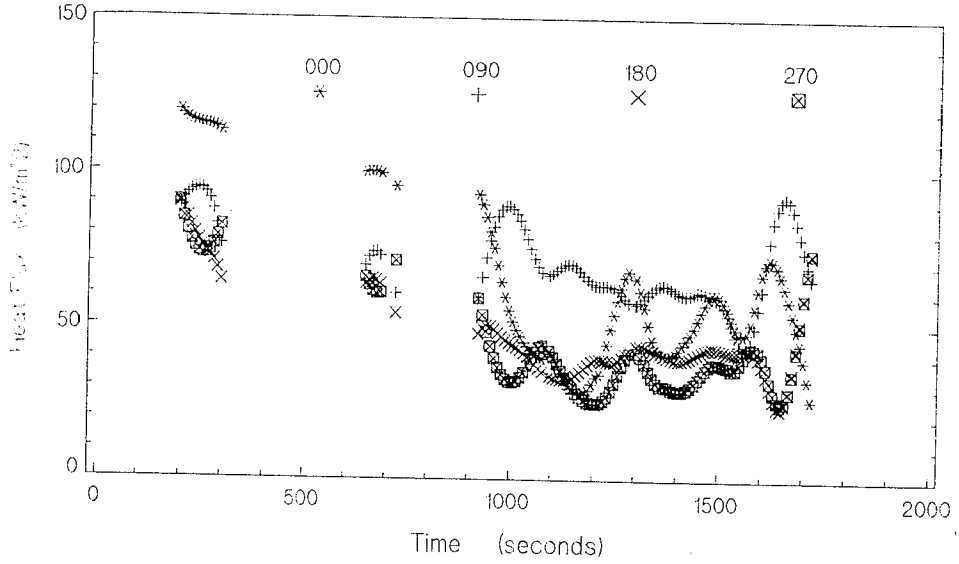

Figure 18. The conditioned data set for test A. Heat flux versus time averaged over 3 stations. The data is plotted as individual points to emphasize the effect of a conditional analysis. The gaps indicate a flame absent condition.

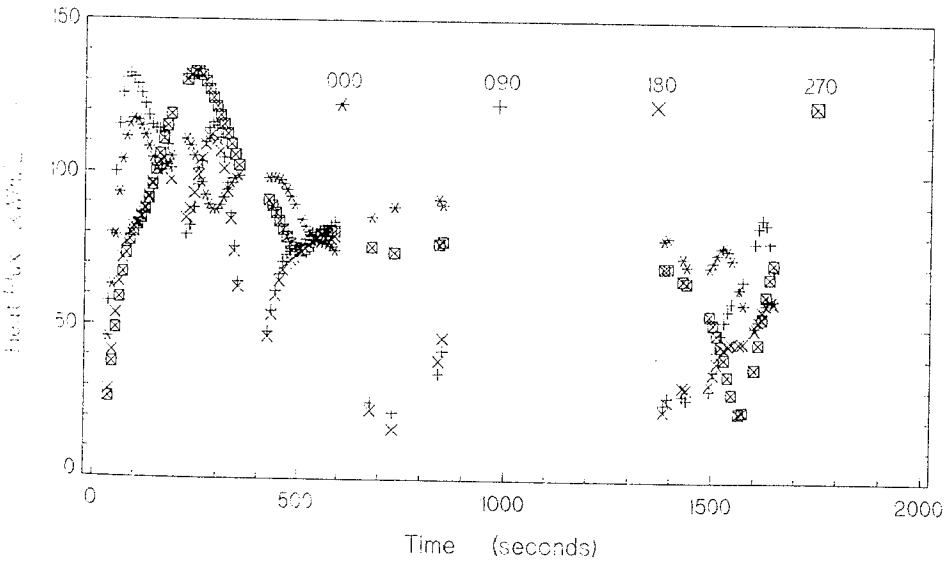

Figure 19. The conditioned data set for test B. Heat flux versus time averaged over 3 stations.

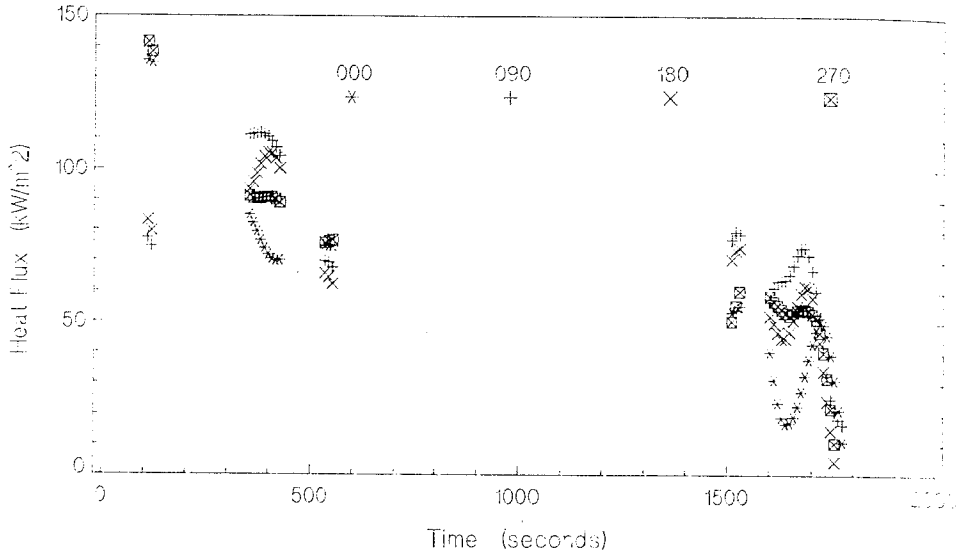

Figure 20. The conditioned data set for test C. Heat flux versus time averaged over 3 stations.

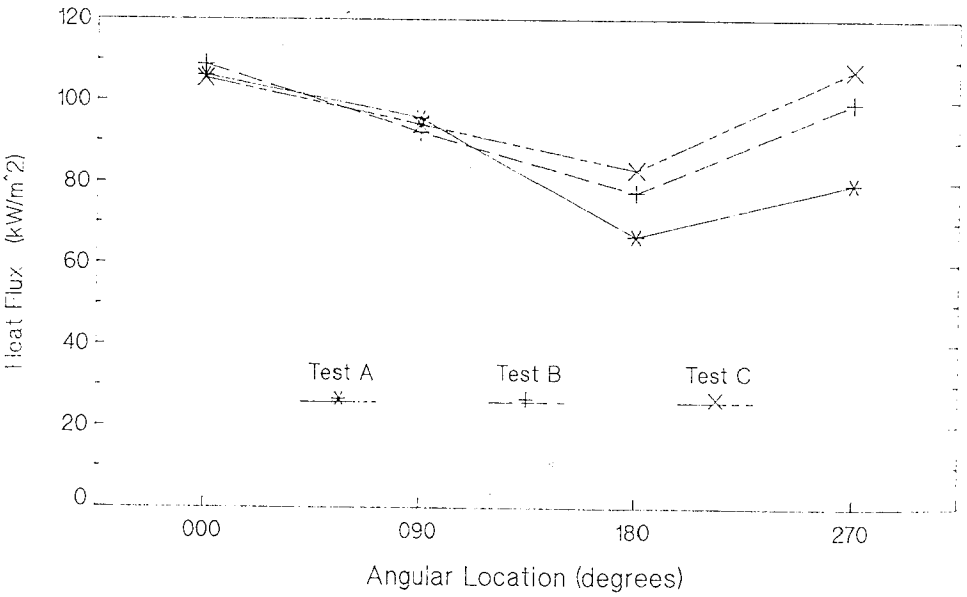

Figure 21. Average total heat flux versus angular location for all tests after applying a conditional analysis. Note how the value for 90 degrees has been increased to a level similar to 270 degrees.

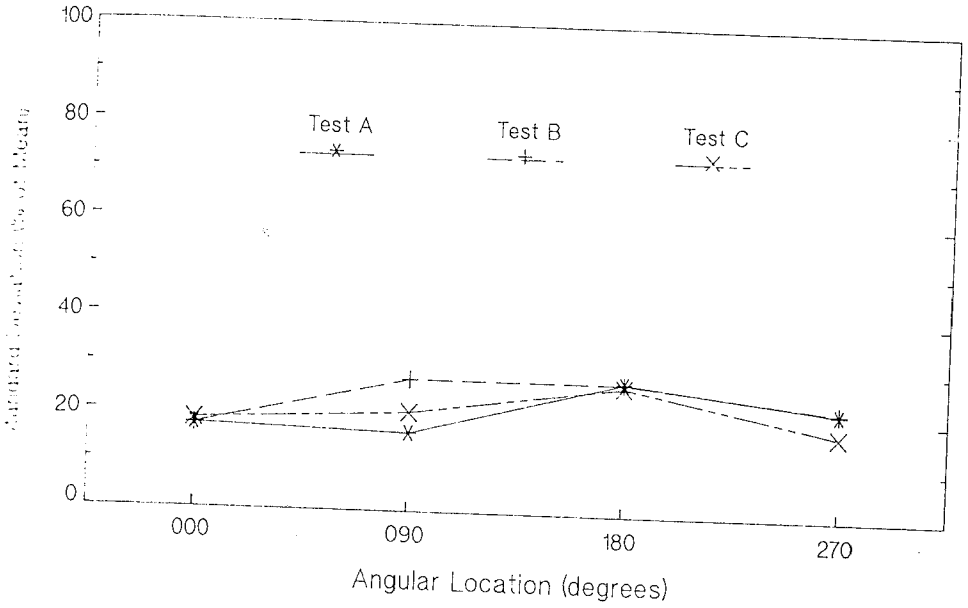

Figure 22. Standard deviation of the average total heat flux after applying a conditional analysis.

It is somewhat surprising that the test statistics are so similar between the three tests, considering the large variance in the original data sets. The mean total heat flux values for locations 0 and 90 are almost identical, although the data does diverge at 180 and 270. This 'collapsing' of the data is another example of the utility of conditioning.

Conclusions

The thermal environment for a physically large, thermally massive object has been measured in a series of large pool fires. Tower and calorimeter based measurements indicate the large scale fluctuations that are induced by even low velocity winds can mask variations in heat flux as a function of location. The comparison between experimental data and simplified models of the fire becomes difficult.

A conditional analysis has been used to examine the distribution of temperatures and heat flux levels during periods of lower wind velocities. The resulting data set has a much lower variance for locations particularly susceptible to wind effects and the test to test variation is also reduced. Additionally, the total heat flux distribution around the large calorimeter becomes much more symmetric and allows an examination the distribution of heat

flux with location. The technique has also been used successfully in the examination of tower temperatures and fire velocity distributions.

In spite of the large, wind induced variations, average total heat flux exceeded the levels specified in the test regulations for radioactive material shipping containers. This was true for all locations on the large calorimeter.

Acknowledgments

The authors would like to express their appreciation for the work of J. J. Gregory in the original data analysis. The test program was funded by the Federal Rail Administration of the U.S. Department of Transportation(DOT). This project was directed by the Transportation Technology Center at Sandia National Laboratories. Sandia National Laboratories is operated by AT&T Technologies for the U.S. Department of Energy(DOE) under contract DE-AC04-76DP00789.

References

1. Standard Methods of Fire Tests of Building Construction and Materials, 1986 Annual Book of ASTM Standards, E 119-83, vol. 4, pp. 353-379.
2. Safety Standards for the Packaging of Fissile and Other Radioactive Materials, United States Energy Research and Development Administration(ERDA) Manual, Chapter 0529, vol. 0000 General Administration, part 0500 Health and Safety.
3. Code of Federal Regulations, Title 49 Transportation, part 173.399, p. 274.
4. Packaging of Radioactive Materials for Transport and Transportation of Radioactive Material Under Certain Conditions, Title 10, Code of Federal Regulations, Part 71, August 19, 1977.
5. Regulations for the Safe Transport of Radioactive Materials, Safety Series No. 6 of International Atomic Energy Safety Standard, 1973 revised edition, IAEA, Vienna, STI/PUB/323.
6. Proposed Test Methods for Determining Effects of Large Hydrocarbon Pool Fires on Structural Members and Assemblies, 1986 Annual Book of ASTM Standards, P 191, vol. 4, pp. 1238-1260.
7. J. J. Gregory, R. Mata, and N. R. Keltner, Thermal Measurements in a Series of Large Pool Fires, SAND85-0196, Sandia National Laboratories, Albuquerque, New Mexico, 1987.
8. B. F. Blackwell, R. W. Douglas, and H. Wolf, A User's Manual for the Sandia One-Dimensional Direct and Inverse Thermal(SODDIT) Code, SAND85-2478, Sandia National Laboratories, Albuquerque, New Mexico, 1985.
9. P. T. Harsha, W. N. Bragg, and R. B. Edelman, A Mathematical Model of a Large Open Fire, Science Applications Incorporated, NASA Contract Report No. NAS2-10675.
10. R. C. Corlett, Velocity Distributions in Fires, in: Heat Transfer in Fires, John Wiley and Sons, New York, 1974, pp. 239-255.
11. A. M. Birk, and P. H. Oosthuizen, Model for the Prediction of Radiant Heat Transfer to a Horizontal Cylinder Engulfed in Flames, ASME Paper 82-WA/HT-52, 1982.
12. M. E. Schneider, and L. A. Kent, Measurements of Gas Velocities and Temperatures in a Large Open Pool Fire, SAND87-0095C, Sandia National Laboratories, Albuquerque, New Mexico, 1987, (to be presented at the 1987 ASME Heat Transfer Conference, Pittsburgh, PA.)